On the Creep Behavior of Auto Glasses at High Temperatures

Ju bing Chen[*], Kai yang Xiao and She xu Zhao

Department of Engineering Mechanics, Shanghai Jiaotong University, Shanghai 200240, China

(Received April 7, 2010; final form April 12, 2010)

ABSTRACT

The experiments of a creep for auto glasses at high temperatures and different stress levels are conducted. It reveals nonlinear deformation behaviors of auto glass at those temperatures. Univer different temperatures and loadings, the creep curves occur in similar shapes. The primary creep is not obvious, but the steady and accelerating creep processes are dominant. And all fracture data follow the Monkman-Grant relationship, not influenced significantly by temperatures and stresses. Based on the experiments, this paper presents a nonlinear constitutive equation to describe the creep of glasses. It is found in comparison the theoretical prediction with experimental data that the nonlinear uniaxial constitutive equation proposed here is able to better describe the creep process of auto glasses at high temperatures.

Keywords: auto glass, high temperature creep, nonlinear constitutive equation

1. INTRODUCTION

Auto glasses are widely used in automobile industry due to their high temperature resistance, high strength, abrasive resistance, and high photostability. Usually, auto glasses are made by using a high temperature treating equipment in which glass will produce high temperature creep .This process directly affects the quality of an auto glass. In engineering applications, therefore, it is important to investigate the characteristics of auto glasses in high temperature creep.

In definition, creep is a tendency of a solid material to slowly move or deform permanently under the circumstances of a stress or temperature. It involves a mechanical property variation of materials with time /1/. Glass is one of common inorganic non-metallic materials, but less described for its creep behaviors in a high temperature. In order to investigate its creep, some researchers established a physical model of deformation for depicting the anelastic and viscoplastic behaviors at high temperatures, and conducted the classical creep and recovery tests with glassy materials near T_g /2/. For three oxynitride glasses with Y-Si-Al-O-N elements, especially, its creep was studied in the temperature range between 1073 and 1273 K, and their viscosities were measured using a three-points bending test at the glass transition domain /3/. Furthermore, the creep

---

[*] Corresponding author: Tel: 86-021-54743061; E-mail address: jbchen@sjtu.edu.cn

curves of the glasses were regressed from experimental data in a tension or compression situation at 623~953 K using a RJY-1 thermo-mechanical tester, and their corresponding viscoelastic parameters were obtained /4/. Recently, the fivefold symmetric icosahedral structure of glass was firstly found in experiments on a colloidal liquid-gel transition / 5/.

For description of the stress-strain variation of organic glasses with time, a viscoelastic creep model was built on the base of shear creep tests under different stresses at 353K /5/. The corresponding theoretical results could give better agreement with the experimental data on creep and recovery, relaxation and deformation at constant strain rates. The steady creep rate and effective stress were described in a power law /6/. For organic glasses, the craze damage in PMMA might take place in the creep. The craze process of PMMA was then observed with an optical microscope. By defining the effective stress in damaged PMMA, the stress-strain relationship of a damaged area was derived. Mechanical properties in damage evolution were studied using a macro-description method combined with a meso-scale investigation /7/. Nevertheless, the accelerating process was not yet considered in all of models mentioned above.

In glass creep hypotheses, high temperature plastic deformation in glasses is in consequence of local shear transformations nucleated through a cooperative movement of atom groups or structural units in a micro-domain /1/, and rearrangements of flow units taking place in a quasi-fixed structure are responsible for the deformation /3/. One will argue that the particle motions with flow can be represented by thermally activated transitions across an energy barrier /4/. Besides, the reduction in a free volume increases inner particle interactions, which leads to a decrease in mobility of the kinetic units /5/.

In this paper, it is identified from the experiments that both high temperature fracture time and steady rate follows the Monkman-Grant relationship, just like crystalline materials /8/. Furthermore, a nonlinear high temperature constitutive relationship is built according to creep characteristics in high temperature creep tests. Finally, it is found that the theoretic prediction calculated on the basis of nonlinear high temperature constitutive equation is better in agreement with experimental data.

2. EXPERIMENTAL

2.1 Experimental devices

Electronic high-temperature stress-rupture testing machine is used in the present experiments. The deformation of materials is measured by a tension rod extensometer, whose traveling distance is 150mm and moving speed 0.05mm~100mm/min. The temperature in furnace is about 473~1273K. **Figure 1** shows a chuck and a glass specimen. The specimen is rectangular in cross-section, and its length, width, and height are 50mm, 9mm and 4mm, respectively.

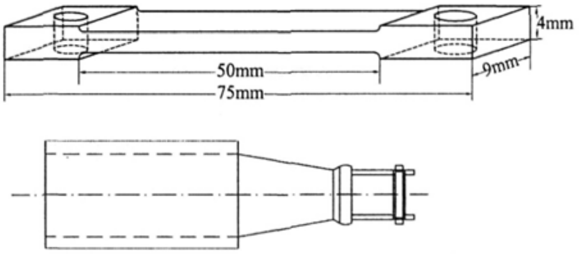

Fig. 1: Specimen and chuck

Chemical compositions of the specimen are shown in **Table 1**.

Table 1

Chemical compositions of the glass (mass%)

SiO_2	Al_2O_3	CaO	Fe_2O_3	MgO	Na_2O+K_2O	SO_2
72.3	1.25	8.01	0.08	4.0	14.0	0.25

1.2 Experimental procedure

The specimen is fixed at the tension rod extensometer and put in furnace at different high temperatures. Temperature, stress and time can be set by experimental program –P&Ctest_P10C. The experimental temperature is set up one by one to 823, 833, 838, 843 and 863 K, and stress applied in experiments is 2MPa, 3.5MPa and 5MPa, respectively.

3. RESULTS AND DISCUSSION

3.1 Creep curves

The creep strain varying with time at different temperatures and stresses are plotted from **Figure 2** to **Figure 6**.

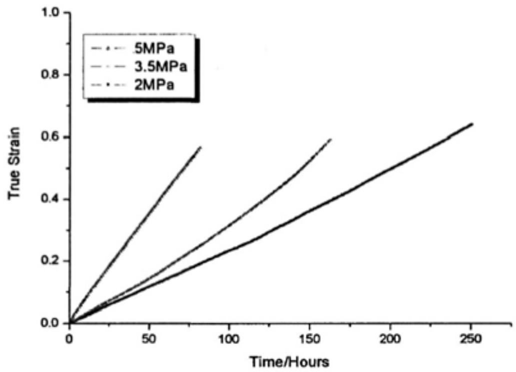

Fig. 2: Test curves of creep at 823K

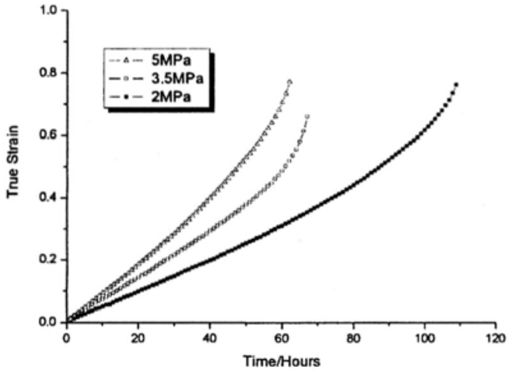

Fig. 3: Test curves of creep at 833K

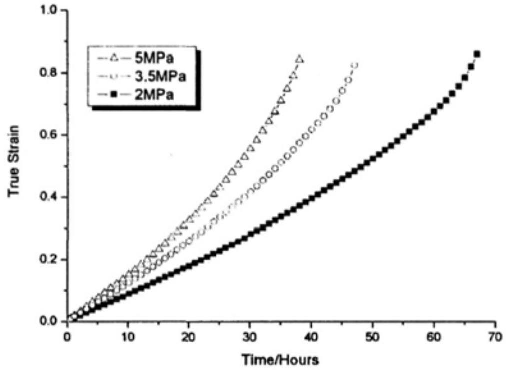

Fig. 4: Test curves of creep at 838K

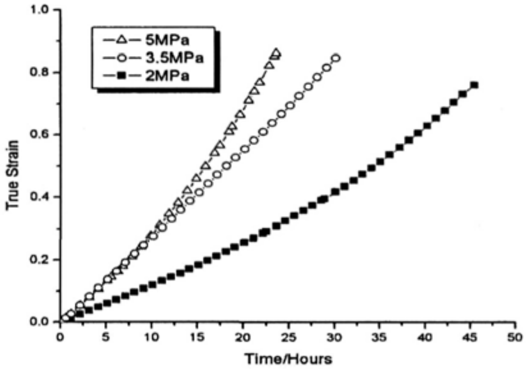

Fig. 5: Test curves of creep at 843K

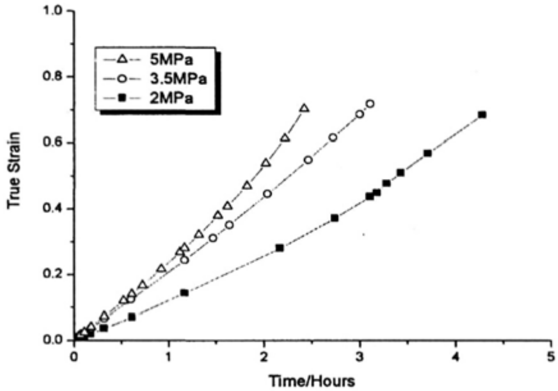

Fig. 6: Test curves of creep at 863K

Taking large deformation of the glass at high temperatures into account, the creep strains in the figures are real values ($\varepsilon=\int\frac{dl}{l}$). It is noted from the above figures that all creep curves at different temperatures and loadings are similar in shape. The transient creep stage is nearly nonexistent, and the primary stage is very short in the whole creep period.

Like metal materials, the steady creep of glassy ones displays a quasi-linear curve, and keeps the longest period in the creep. At the final stage of the creep, it speeds up until rupture.

The experimental results indicate that the strain is a function of both stress and temperature, intensifying with the increase of stress and temperature. The slope of the curves at the steady creep stage gradually becomes larger and its creep period gets shorter with the increase of stress or temperature. The steady creep stage is quite long related to the whole creep period. The increase of both stress and temperature enlarges the creep strain, but decreases the creep period. In addition, variations of the creep strain are between 0.6~0.9. Summarily, it is significant characteristics of a glass creep under the circumstances of stress and high temperature that after a short primary stage, the creep experiences a long term steady stage, and finally creep speeds suddenly up gives rise to a largest strain until rupture.

3.2 The effect of temperature and stress for creep rate

3.2.1 The effect of temperature

Given the stress (σ=3.5MPa), the variation of $\dot{\varepsilon}_c$ with respect to t / t_f is plotted in **Figure 7**, where $\dot{\varepsilon}_c$ is creep rate, t / t_f a normalized time, and t_f the creep fracture time. The figure reveals that the increase of temperature leads to the creep rate rise and decrease the steady-state creep stage. **Figure 8** shows that steady creep rate become more nonlinear with the rise in temperature.

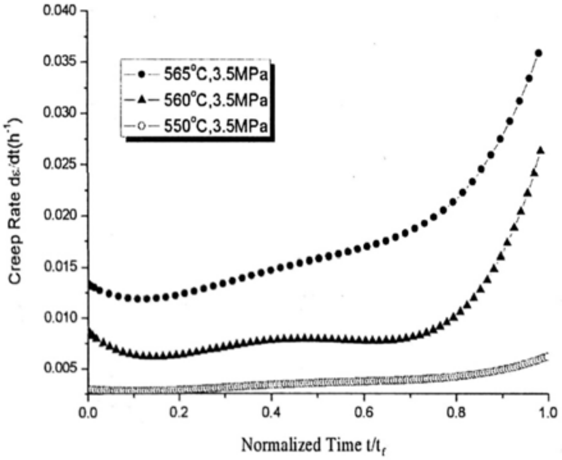

Fig. 7: Effect of temperature on creep rate

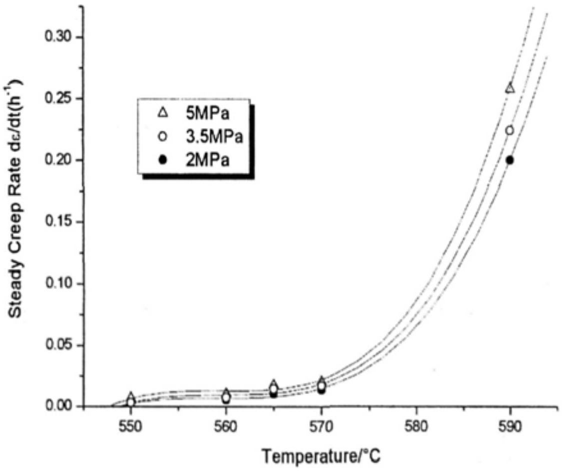

Fig. 8: Effect of temperature on steady creep rate

3.2.2 The effect of stress

In the same way, at the temperature (838 K), the variation of $\dot{\varepsilon}_c$ with respect to t / t_f is plotted in **Figure 9**; and the stresses are exerted 2MPa, 3.5MPa and 5MPa, respectively. **Figure 9** demonstrates that with the growth of stress, the creep rate increases, and the steady-state creep stage becomes short. The steady creep rate against stress is drawn in **Figure 10**. It shows that the steady creep rate becomes slowly large as stress rises.

3.3 Monkman-Grant relationship

Monkman-Grant number indicates a connection between materials fracture time and steady creep rate, fracture can be determined of a material at the steady

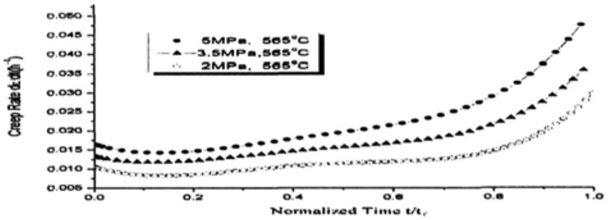

Fig. 9: Effect of stress on creep rate

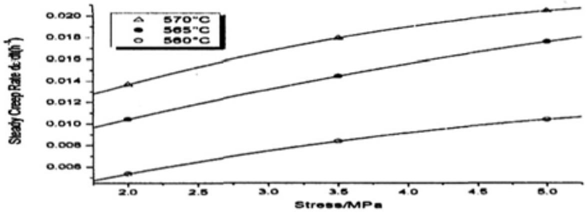

Fig. 10: Effect of stress on steady creep rate

creep stage. Therefore, the corresponding information can be derived by determination of Monkman-Grant number. The expression of Monkman-Grant number is given by

$$t_f \cdot \dot{\varepsilon}_m = C_{MG} \tag{1}$$

where C_{MG} is the Monkman-Grant number, t_f the fracture time, and $\dot{\varepsilon}_m$ the steady creep rate.

According to the aforementioned creep test data at high temperature, when given the stress (for example, σ=5MPa) or temperature (838K), the Monkman-Grant number can be calculated as shown in **Tables 2 and 3.**

Table 2

Monkman-Grant constant (σ=5MPa)

Temperature / K	t_f / h	$\dot{\varepsilon}_m / h^{-1}$	C_{MG}
823	88	0.00691	0.6081
833	62	0.01039	0.6442
838	38	0.01757	0.6676
843	30	0.02042	0.6126
863	2.42	0.25790	0.6241

Table 3

Monkman-Grant constant at 838 K

Stress /MPa	t_f / h	$\dot{\varepsilon}_m / h^{-1}$	C_{MG}
2	38	0.01043	0.6881
3.5	47	0.01443	0.6721
5	66	0.01757	0.6676

Seen from the two tables, the value of Monkman-Grant number is not influenced significantly by temperatures and stresses, and it varies from 0.6081 to 0.6881.

3.3 A nonlinear constitutive relationship

3.3.1 The establishment of constitutive relation

One usually assumes that the creep rate is a separable function of three independent variables, i.e. temperature (*T*), stress (*σ*), and structure factor (*S*). The structure factor is thought to involve the effects of relevant structural variables, and these variables are functions of the strain /9/. The creep rate is then represented as

$$\dot{\varepsilon} \propto f(T) \cdot f(\sigma) \cdot f(S) \tag{2}$$

Rouxel /3/ has argued that the creep deformation of glass results from the reagrrangements of flow units taking place in a quasi-fixed structure with a quasi-fixed free volume distribution. These transformations can be thermally activated under exerted stresses, and their kinetics can be treated with the standard procedure of the transtion state theory, a macroscopic creep rate is below

$$\dot{\varepsilon}_c^{st} = A\sigma^n e^{-\frac{Q_c}{RT}} \tag{3}$$

where $\dot{\varepsilon}_c^{st}$ is the steady creep rate (h^{-1}), *A* a constant for a given material, σ the applied stress (MPa), *n* average stress exponent, Q average apparent activation energy

(KJ/mol), R gas constant, and T absolute temperature (K).

Glass is a non-crystalline material, and its internal structure will change significantly as the temperature is up to the transitional point T_g. The change would have great influence on the creep rate at high temperature, and therefore, Eq. (3) can be modified as

$$\dot{\varepsilon}_c^{st} = A\sigma^n \mathrm{e}^{-\frac{Q_c}{RT}} \left(\frac{T}{T_g}\right)^{\gamma_c} \tag{4}$$

Where $\left(\frac{T}{T_g}\right)^{\gamma_c}$ represents an effect of change of internal structure glass on the steady creep rate, γ_c structure effect exponent of the steady creep. The transition temperature T_g can be obtained by the experiment.

The integration of Eq. (4) with respect to t gives

$$\varepsilon_c^{st}(\sigma,T,t) = B\sigma^n \mathrm{e}^{-\frac{Q_c}{RT}} \cdot \left(\frac{T}{T_g}\right)^{\gamma_c} \cdot t \tag{5}$$

where B is a corresponding material constant.

In consideration of the response characteristics at the primary stage, the constitutive relation at the primary stage is constructed as

$$\varepsilon_c^{in}(\sigma,T,t) = A\sigma^n \mathrm{e}^{-\frac{Q_c}{RT}} \cdot \left(\frac{T}{T_g}\right)^{\gamma_c} \cdot \left(1-\mathrm{e}^{-kt}\right) \tag{6}$$

where $\varepsilon_c^{in}(\sigma,T,t)$ is a strain function at the primary stage, k denotes a material constant.

When t/t_f becomes larger at the accelerating stage, the creep rate accordingly speeds up until fracture. For a crystalline material, the fracture creep time and steady creep rate follow a reciprocal relation /8/, and fracture time depending on temperature and stress is described as

$$t_f = D\sigma^m \mathrm{e}^{\frac{Q_f}{RT}} \tag{7}$$

where D is a material constant, m an average stress exponent of the fracture time, Q_f average fracture activation energy (kJ/mol).

According to the experimental data and the Monkman-Grant relationship, the expression of the fracture time at high temperature is written as

$$t_f = D\sigma^m \mathrm{e}^{\frac{Q_f}{RT}} \left(\frac{T}{T_g}\right)^{-\gamma_c} \tag{8}$$

Based on the response characteristic at the accelerating stage and Eq.(8), the constitutive relation at the accelerating stage is determined using the following equation

$$\varepsilon_c^{ac}(\sigma,T,t) = C\sigma^n \mathrm{e}^{-\frac{Q_c}{RT}} \cdot \left(\frac{T}{T_g}\right)^{\gamma_c} \cdot \left(\mathrm{e}^{f(\sigma,T,t)}-1\right) \tag{9}$$

$$f(\sigma,T,t) = \frac{t}{D\sigma^m \mathrm{e}^{\frac{Q_f}{RT}} \left(\frac{T}{T_g}\right)^{-\gamma_c}}, \tag{10}$$

where C and D are corresponding to material constants.

Finally, from Eqs. (4) ,(5) and (6) , the nonlinear constitutive relation suitable for the whole period is built up

$$\varepsilon_c(\sigma,T,t)=\sigma^n \mathrm{e}^{-\frac{Q_c}{RT}}\cdot\left(\frac{T}{T_g}\right)^{\gamma_c}\cdot\left[A\left(1-\mathrm{e}^{-kt}\right)+Bt+C\left(\mathrm{e}^{f(\sigma,T,t)}-1\right)\right] \tag{11}$$

3.3.2 Parameters determination

After taking the natural logarithm of equation (3), the following equation can be derived

$$\ln\dot{\varepsilon}=\ln B+n\ln\sigma-Q_c/RT \tag{12}$$

When Plotting a curve of $\ln\dot{\varepsilon}$ against $1/K$, its slope gives the activation energy. Furthermore, Q_c can be obtained after averaging different activation energies. Similarly, when plotting $\ln\dot{\varepsilon}$ versus $\ln\sigma$, n can be calculated from the slope of the curves. All of the results are shown in **Figure 11** and **Figure 12**.

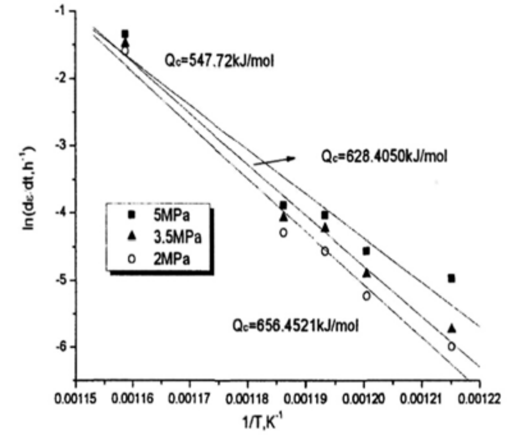

Fig. 11: Apparent activation energy at different stress levels

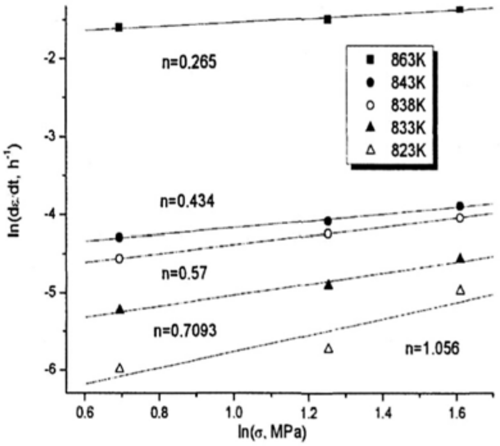

Fig. 12: Stress exponents at different temperatures

Here, Q_f and m can be determined by a simple calculation. And other corresponding material constants can be obtained by using the least square method, as shown in **Table 4**. Obviously, the average apparent activation energy is greater than the average fracture activation energy. It indicates the capacity of anti-creep at the steady stage is stronger than the creep resistance at the accelerating stage. For this reason, duration is longer at the steady stage. Theoretical prediction can be made after substituting all material parameters in **Table 4** into nonlinear constitutive relation (11).

Table 4

Material parameters

A	B	C	D	k
0.00132	0.00529	0.00571	34.4947	0.0169

m	n	Q_c (kJ/mol)	Q_f (kJ/mol)	γ_c
-0.7333	0.609	610.86	580.615	49.8204

3.3.3 Numerical prediction

Comparisons between experimental data and theoretical prediction are plotted in **Figure 13** to **Figure 17**. It is found the figures that the primary stage, described by creep response curves, is not obvious. But

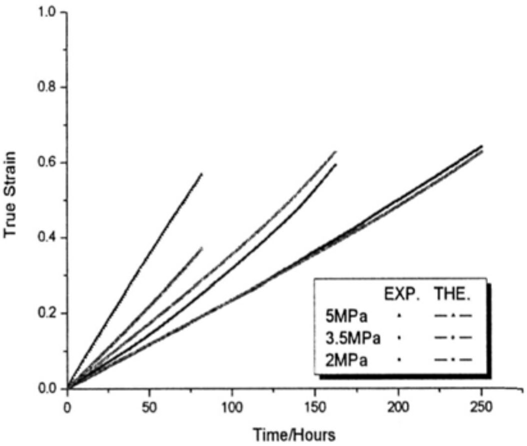

Fig. 13: Curves of creep at 823K

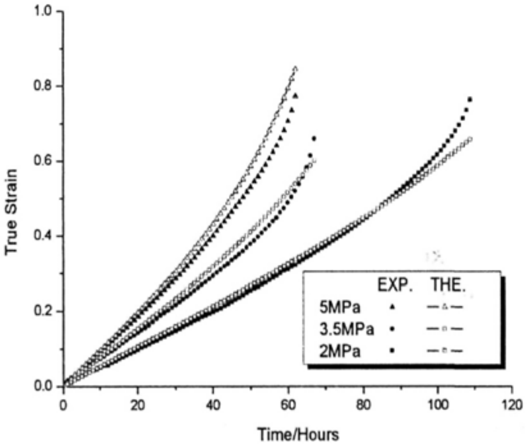

Fig. 14: Curves of creep at 833K

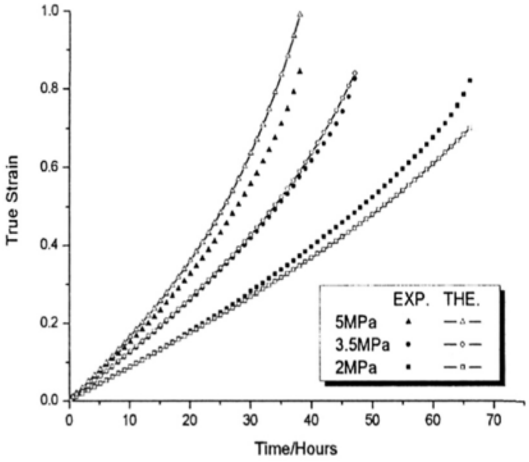

Fig. 15: Curves of creep at 838K

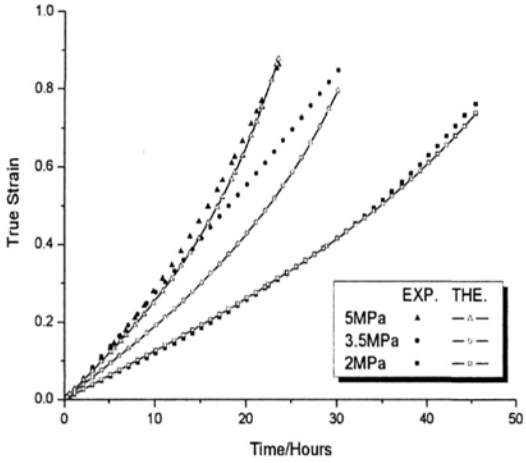

Fig. 16: Curves of creep at 843K

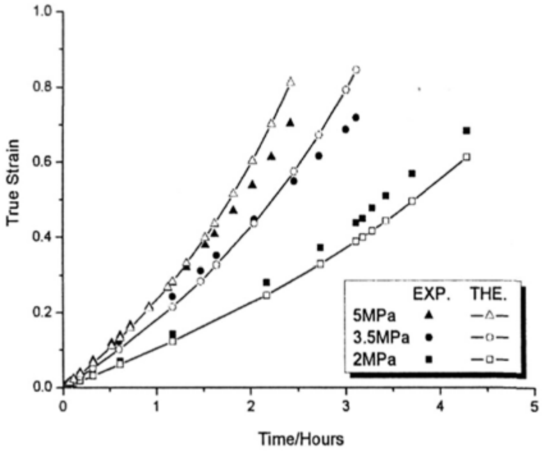

Fig. 17: Curves of creep at 863K

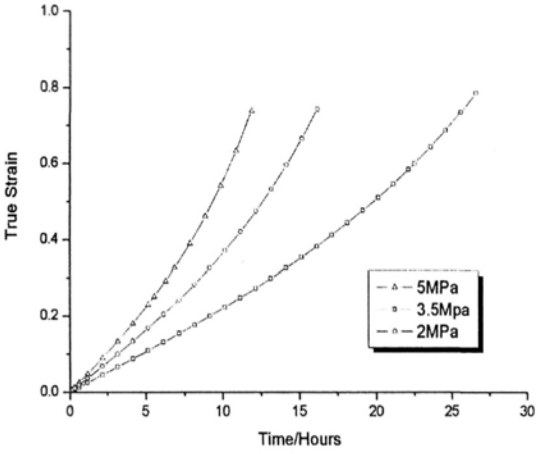

Fig. 18: Curves of creep at 848K

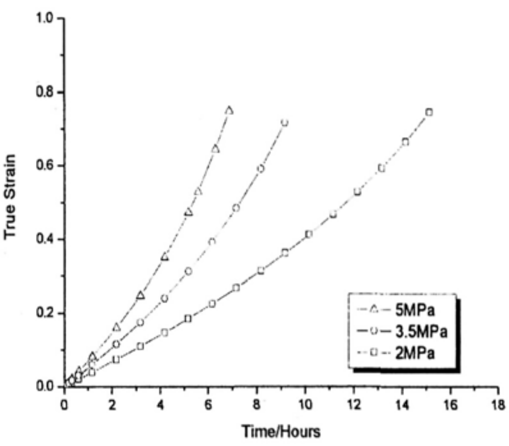

Fig. 19: Curves of creep at 853K

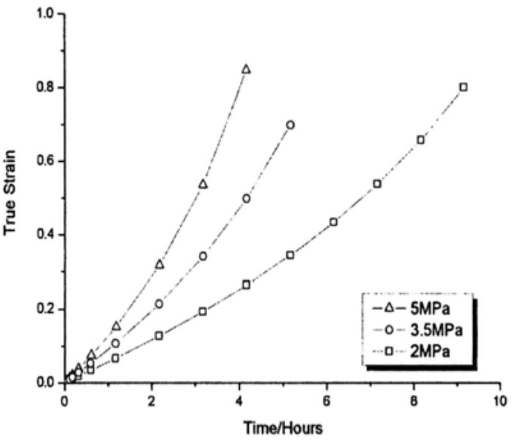

Fig. 20: Curves of creep at 858K

at the steady stage, the theoretical curves have good agreements with experimental data, especially in the cases of temperature at 848K, 853K, and 858K shown in **Figure 18** to **Figure 20**.

4. CONCLUSIONS

The creep of auto glasses has the same characteristics as those of the crystalline materials. The primary stage of creep is very short, submersed in the whole process and often neglected. But the steady stage is dominant, and with the increase of temperature or stress, it would become short. At the acceleration stage, with lapse of time the creep strain and rate increase rapidly until fracture happens.

At the steady stage, with the increase of temperature and stress the strain increases, and the stage would become shorter and shorter. In addition, at the stage the creep rate changes rapider and rapider with the increase of temperature, but a little bit insensitive to the stress change.

Just like crystalline materials, the fracture of glass obeys a criterion from Monk-Grant number.

The nonlinear constitutive equation presented here can describe the behavior of high temperature creep of glass.

ACKNOWLEDGEMENT

This research work was supported by National Natural Science Foundation of China, No.10772117and No. 10872130.

REFERENCES

1. X.Y. Mu, *Creep Mechanics*, Xi'an Jiaotong University Press, Xi'an (1990), (in Chinese).
2. C.Borde, C .Mat and J. Perez. *J. of Non-Cryst. Solids*, **56**, 399-404(1983).
3. T.Rouxel, M.Huger and J .L .Besson, *J. of Mater. Sci.*, **27**, 279-284(1992).
4. Mao Qizhao Wang Qihong Shan Junhong and L Feng. *J. of Chinese Ceramic Society*, **25**, 18-23(1997). (in Chinese)
5. O. E. Ol'khovik and N.P. Demenchuk, *Porblemy prochnosti*, **2**, 49-55 (1977)
6. N .T .Smotrin and V. M. Chebanov, *Polymer mechanics*, **1**, 60-66(1965).
7. J.Q. Chen, T.P. Li, Zh.D. Li and T.Q. Yang. Mechanical science and technology. **2**, 371~374(2006). (in Chinese)
8. J. T. Guo, C. Yuan, H. C. Yang, V. Lupinc and M. Maldini, *Metallurgical and Materials Transaction A*, **32A**, 1103-1110 (2001).
9. E. M. Heuse and G. Partridge. J. of Mater. Sci., 9, 1255-1261(1974)